Simulation of Hydrogen/Air Laminar Diffusion Flame

by

Seishiro FUKUTANI and Hiroshi JINNO

(Received March 30, 1988)

Department of Industrial Chemistry, Faculty of Engineering, Kyoto University, Yoshida, Sakyo-ku, Kyoto 606, Japan

Abstract

A model as precise as possible both from chemical reactions and fluid mechanics was constructed and applied to simulate a laminar hydrogen/air diffusion flame. The combustion conditions were given as that the burner is 10 mm in diameter, and hydrogen issues with the Poiseuille flow with 10 ml/s of the axial volumetric velocity. The obtained results were as follows. The flame is well-developed as a typical diffusion flame at about 10 mm in height. At this height, the flame-sheet assumption is valid. On the contrary, hydrogen atoms diffusing axially from a downstream region, and oxygen entrained with the radial flow of the environmental air, react at a height as low as 2 mm. This reaction produces hydroperoxyl radicals and releases a fairly large amount of thermal energy at the same time. Thereby, enthalpy is carried to the upperstream region in the form of chemical energy. The flame holding of this flame can be ascribed to these low-temperature reactions.

1. Introduction

Except for a few pioneering works by Miller and Kee[1], for instance, most of the fundamental researches on diffusion flames have been done assuming the flame-sheet model proposed by Burke and Schumann[2]. Furthermore, chemical reactions are often replaced by a single overall reaction and treated only as a heat-releasing step.

In premixed flames, however, chemical reactions take place with various reaction mechanisms depending on the gas composition and the temperature. A similar situation should be observed even in a diffusion flame. A precise model which includes a full reaction scheme and many species is thus expected to yield detailed information on the structure of a diffusion flame such as the distributions of temperature, the species concentrations and the rates of chemical reac-

tions.

On the other hand, the mechanism of flame holding is interesting as is a flame structure. The flame holding of a diffusion flame is simply explained as premixed gas produced partly by the interdiffusion of fuel and air at the base of a flame. It burns in a fairly short time just like a premixed flame, and pulls down the whole flame toward a burner[3]. The precise model can be used for the detailed investigation of that mechanism.

In this investigation, a mathematical model for an axisymmetric diffsion flame is constructed and applied to investigate the flame structure of a hydrogen /air diffusion flame and the mechanism of flame holding. A hydrogen/air diffusion flame includes not only the fuel with a large diffusion coefficient, but also hydrogen atoms having the largest diffusion coefficient as an intermediate. It may, therefore, exhibit the typical properties of diffusion flames.

2. Mathematical Model

A mathematical model for diffusion flames was constructed on the basis of the following assumptions:

1. The flame under consideration contains nine species, OH, H, O, HO_2, H_2O_2, H_2, O_2 and N_2. Twenty-one elementary reactions may occur among these species as tabulated in Table 1. Nitrogen is inert and acts only as a third body in recombination reactions.
2. Heat transfer from the flame to its surroundings is neglected. Radiative heat transfer inside the flame is also neglected.
3. The flame is axially symmetric. The governing equations are expressed like Eqs. (1) - (6) in the cylindrical coordinates.

$$\frac{\partial \rho}{\partial t}+\frac{1}{r}\cdot\frac{\partial}{\partial r}(\rho u r)+\frac{\partial}{\partial z}(\rho v)=0 \tag{1}$$

$$\rho\left(\frac{\partial u}{\partial t}+u\frac{\partial u}{\partial r}+v\frac{\partial u}{\partial z}\right)$$
$$=\frac{\partial}{\partial r}\left(\mu\left(2\frac{\partial u}{\partial r}-\frac{2}{3}\left(\frac{1}{r}\cdot\frac{\partial}{\partial r}(ur)+\frac{\partial v}{\partial z}\right)\right)\right)$$
$$+\frac{\partial}{\partial z}\left(\mu\left(\frac{\partial u}{\partial z}+\frac{\partial v}{\partial r}\right)\right)+\frac{2\mu}{r}\left(\frac{\partial u}{\partial r}-\frac{u}{r}\right)-\frac{\partial p}{\partial r} \tag{2}$$

$$\rho\left(\frac{\partial v}{\partial t}+u\frac{\partial v}{\partial r}+v\frac{\partial v}{\partial z}\right)$$

Table 1 H_2/O_2 reaction scheme[a]
$k = A \cdot T^n \cdot \exp(-E/T)$

No.	Reation	A	n	E	Ref.
1.	$H_2+O_2 \rightarrow OH+OH$	2.50E06	0.0	19600.0	4
2.	$H+O_2 \rightarrow OH+O$	2.20E08	0.0	8450.0	4
3.	$O+H_2 \rightarrow OH+H$	1.80E04	1.0	4480.0	4
4.	$OH+OH \rightarrow O+H_2O$	6.30E06	0.0	550.0	4
5.	$OH+H_2 \rightarrow H+H_2O$	2.20E07	0.0	2590.0	4
6.	$H+H+M+ \rightarrow H_2+M$	2.60E06	− 1.0	0.0	4
7.	$O+O+M \rightarrow O_2+M$	1.90E01	0.0	− 900.0	4
8.	$H+O+M+ \rightarrow OH+M$	3.60E06	− 1.0	0.0	5
9.	$OH+H+M \rightarrow H_2O+M$	4.06E10	− 2.0	0.0	4
10.	$H+O_2+M \rightarrow HO_2+M$	5.00E03	0.0	− 500.0	4
11.	$H+HO_2 \rightarrow H_2+O_2$	2.50E07	0.0	350.0	4
12.	$H+HO_2 \rightarrow OH+OH$	2.50E08	0.0	950.0	4
13.	$H+HO_2 \rightarrow O+H_2O$	9.00E05	0.5	2000.0	4
14.	$OH+HO_2 \rightarrow H_2O+O_2$	5.00E07	0.0	500.0	6
15.	$O+HO_2 \rightarrow OH+O_2$	6.30E07	0.0	350.0	7
16.	$HO_2+H_2 \rightarrow H+H_2O_2$	7.30E05	0.0	9400.0	4
17.	$HO_2+HO_2 \rightarrow H_2O_2+O_2$	8.50E06	0.0	500.0	4
18.	$OH+H_2O_2 \rightarrow HO_2+H_2O$	1.00E07	0.0	910.0	4
19.	$H+H_2O_2 \rightarrow OH+H_2O$	2.20E09	0.0	5900.0	4
20.	$O+H_2O_2 \rightarrow OH+HO_2$	2.80E07	0.0	3200.0	4
21.	$H_2O_2+M \rightarrow OH+OH+M$	1.20E11	0.0	22900.0	4

[a]Quantity is expressed in m·mol·s units.

$$= \frac{\partial}{\partial z}\left(\mu\left(2\frac{\partial v}{\partial z} - \frac{2}{3}\left(\frac{1}{r}\cdot\frac{\partial}{\partial r}(ur) + \frac{\partial v}{\partial z}\right)\right)\right)$$

$$+ \frac{1}{r}\cdot\frac{\partial}{\partial r}\left(\mu r\left(\frac{\partial u}{\partial z} + \frac{\partial v}{\partial r}\right)\right) - \frac{\partial p}{\partial z} - \rho g \tag{3}$$

$$c_p\rho\left(\frac{\partial T}{\partial t} + u\frac{\partial T}{\partial r} + v\frac{\partial T}{\partial z}\right)$$

$$= \frac{1}{r}\cdot\frac{\partial}{\partial r}\left(\lambda r\frac{\partial T}{\partial r}\right) + \frac{\partial}{\partial z}\left(\lambda\frac{\partial T}{\partial z}\right)$$

$$+ \sum_i D_i\rho\frac{\partial h_i}{\partial r}\cdot\frac{\partial \omega_i}{\partial r} + \sum_i D_i\rho\frac{\partial h_i}{\partial z}\cdot\frac{\partial \omega_i}{\partial z}$$

$$- \sum_i h_i\phi_i \tag{4}$$

$$\rho\left(\frac{\partial \omega_i}{\partial t} + u\frac{\partial \omega_i}{\partial r} + v\frac{\partial \omega_i}{\partial z}\right)$$

$$=\frac{1}{r}\cdot\frac{\partial}{\partial r}\left(D_i\rho r\frac{\partial\omega_i}{\partial r}\right)+\frac{\partial}{\partial z}\left(D_i\rho\frac{\partial\omega_i}{\partial z}\right)+\phi_i \tag{5}$$

$$p=\rho RT\sum_i\frac{\omega_i}{m_i} \tag{6}$$

where t is time; r, radius; z, axial distance; ρ, the density of a gas mixture; u, the radial flow velocity; v, the axial flow velocity; p, pressure; μ, the viscosity; c_p, the specific heat at constant pressure; T, temperature; λ, the thermal conductivity; D, the diffusion coefficient; h, the enthalpy; ω, the mass fraction; ϕ, the production rate due to chemical reactions; R, the universal gas constant and m, the molecular weight. The subscript i denotes the i-th species.

The viscosity, the thermal conductivity and the diffusion coefficient of the components were estimated using Hirschfelder's, Eucken's and Hirschfelder's approximate equations, respectively[8]. The other thermodynamic data, including the equilibrium constants, which were used to estimate the rate constants of the reverse reactions, were obtained from JANAF data[9].

The set of the partial differential equations was transformed into the corresponding finite difference equations. The differentials regarding the spatial coordinates were discretized according to the control-volume method[10]. Each control volume is surrounded with edges of 1 mm in the axial direction and 0.5 mm in the radial direction. The differentials regarding time were developed to an explicit difference scheme. A set of the finite difference equations was solved iteratively until the time-independent solutions were obtained. The time interval was shifted from 10^{-9} s to 10^{-7} s, depending on the degree of convergence.

An actual burner has a wall with a certain thickness and this wall causes turbulence in a downstream region of a combustible gas mixture. It is widely accepted that the recirculation zone induced by this turbulence plays an important role in flame holding. The effect of burner edges on flame holding is one of the interesting problems to be solved. However, flame holding at burner edges results from the complicated interactions among chemical reactions and fluid mechanics. It is necessary to construct very fine spacemeshes to simulate precisely these interactions. In this investigation, therefore, the simple boundary condition was adopted at the burner side. The boundary conditions are as follows: (1) Hydrogen issues through a cylindrical tube as a well-developed Poiseuille flow with a given velocity. (2) The burner tube has a flange at the mouth so that the environmental air flows only to the radial direction at the burner side. (3) The temperature of the fuel and the air is 298 K at the lower boundary. (4) The gradients of all the dependent variables except the radial

velocity are zero at the upper and the side boundaries. The gradient of the radial velocity is also zero at the upper boundary, but that velocity is proportional to the radius at the side boundary.

3. Results and Discussion

The burner is 10 mm in diameter, and the flow velocity of hydrogen is 10 cm^3/s. The experiment gave a stable diffusion flame under the same combustion condition.

Figure 1 shows the predicted temperature distribution in the hydrogen/air diffusion flame simulated in this investigation. The axial profiles of the temperature along the center line and at 5 mm in radius are shown in Fig. 2. The temperature increases very steeply above the burner wall (r= 5 mm), and reaches 2000 K or more at 4 mm in height. The maximum temperature predicted in this flame is 2330 K, which is observed at the position with r= 5.5 mm and z= 5 mm. The high-temperature region, which is defined as the region with

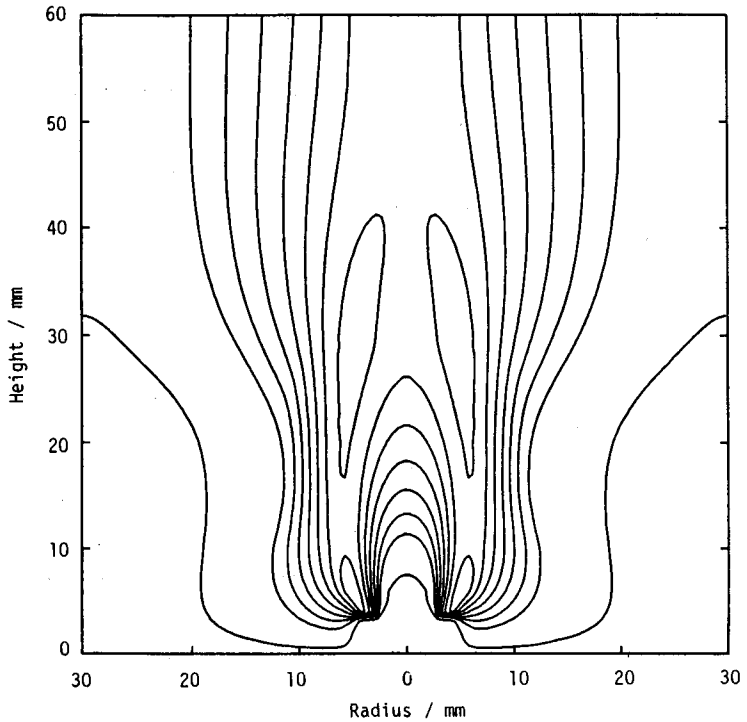

Figure 1. Distribution of temperature expressed with contour lines of 500 K and every 200 K between 1000 K and 2200 K.

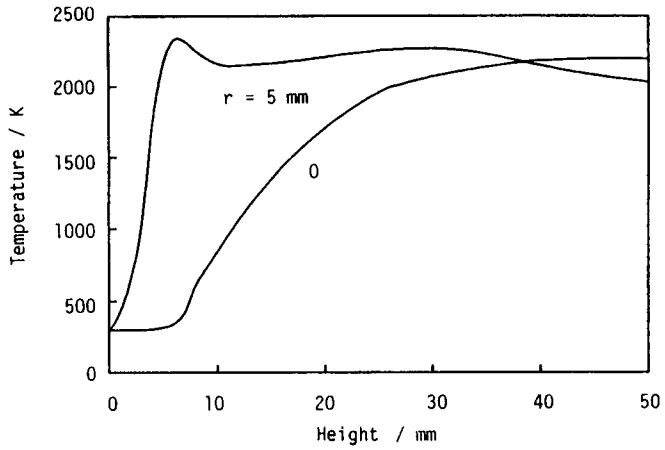

Figure 2. Axial profiles of temperature.

a temperature higher than 2000 K, is extended at the radius a little larger than that of the burner. The thickness of this region is about 3 mm at the base of the flame and increases toward the center line with increasing height. The temperature is raised up to more than 2000 K at about 25 mm in height along the center line. Its distribution becomes fairly flat above 40 mm in the vicinity of the center line. The region having a temperature higher than 1000 K, on the other hand, is extended to more than 10 mm in radius even at the height of 3 mm from the burner. This rapid extension of the flame at the base is observed also in the experiments, though the boundary conditions at the burner side, especially the temperature at the flange surface, are not necessarily the same as each other.

Figure 3 gives the distributions of the three active species, OH radicals and H and O atoms. Hydroxyl radicals, which predominantly oxidize H_2 into H_2O, are widely distributed. The region where OH radicals are present more than 0.001 in mole fraction roughly overlaps with the region where the temperature is higher than 2000 K and the local equivalence ratio ranges from 0.01 to 100. The local equivalence ratio was estimated on the basis of the concentrations of free hydrogen and oxygen in the gas mixture. Hydrogen atoms are distributed in the region over a wide range of the equivalence ratio due to their mobility. In particular, they are diffused toward the center line and are present even at the base of the flame, where the temperature is as low as 1000 K. On the contrary, the distribution of O atoms is restricted to the narrow region with a temperature higher than 2100 K and the equivalence ratio of around unity. The mole fractions of these three active species are generally large at the base of the flame,

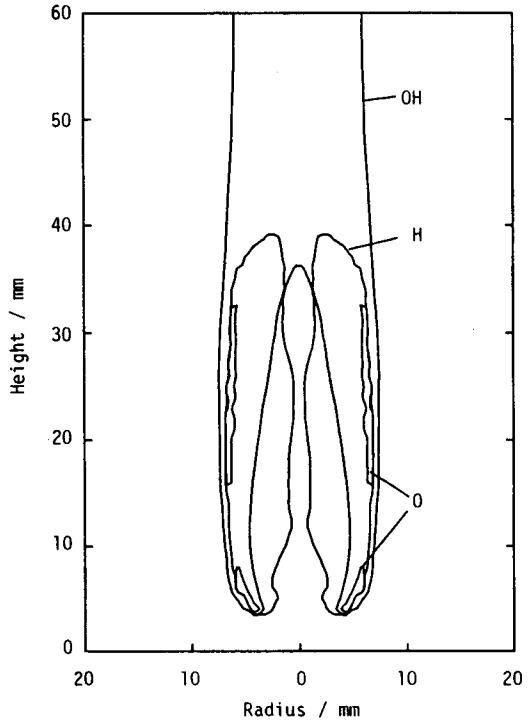

Figure 3. Distribution of concentrations of hydroxyl radicals and hydrogen and oxygen atoms with contour lines of 0.001 in mole fraction.

indicating that chemical reactions are strongly activated there.

A flame front is determined experimentally based on the temperature distribution and/or the concentrations of species, particularly of active species. The location of a flame front does not necessarily agree depending on the definition. It is, therefore, difficult to determine the location of a flame front based only on the results obtained by means of a mathematical model. In addition, the mathematical model proposed in this investigation does not include any heat-loss terms to the surroundings. It may make the location of the flame front in the downstream region different from that in an actual flame. However, it can be concluded that the flame front of the hydrogen/air diffusion flame simulated in this investigation extends from 3 mm to 40 mm in height with a radius of 7 mm.

The flame is well-developed at a height more than 10 mm. There is no essential difference in the flame structure depending on the axial position. The radial profiles of the temperatures and the concentrations of stable species are

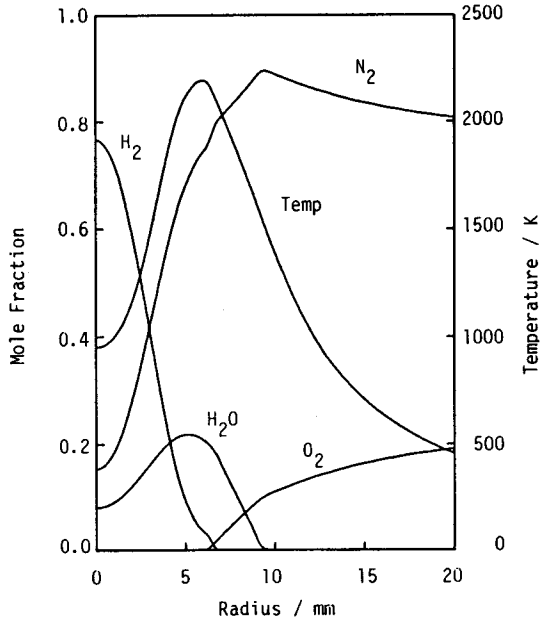

Figure 4. Radial profiles of temperature and concentrations of stable species at 10 mm in height.

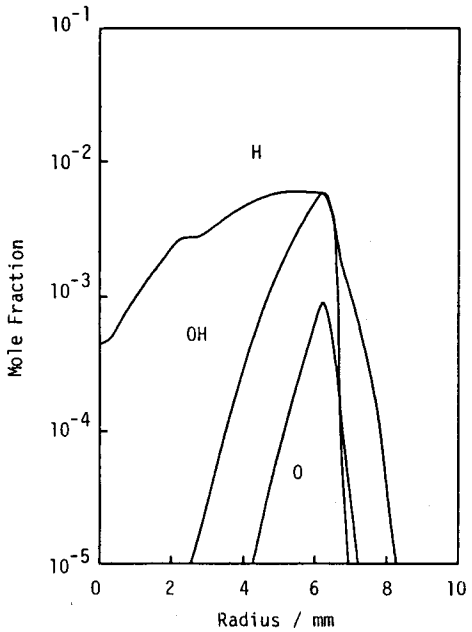

Figure 5. Radial profiles of concentrations of active species at 10 mm in height.

shown in Fig. 4, and those of intermediate species in Fig. 5. Both of the HO_2 radicals and H_2O_2 are present with the mole fractions less than 1 ppm. Hydrogen and oxygen are simultaneously exhausted at about 6 mm in radius. The tempereture and the concentration of water vapor reach their maximum values at almost the same radius. The fuel and the oxidizer are supplied there predominantly with their radial diffusion, and the other contributions are less than 1/10 of the radial diffusion.

The flame front possesses the characteristics as a typical diffusion flame, indicating that the Burke-Schumann model is valid. The region with a temperature higher than 2000 K preferably extends in the rich side with the thickness of about 3 mm, as shown also in Fig. 1.

The predominant reactions at this height are:

$$OH+H_2 \rightarrow H+H_2O, \qquad (H.R\,5)$$
$$H+O_2 \rightarrow OH+O, \qquad (H.R\,2)$$
$$O+H_2 \rightarrow OH+H, \qquad (H.R\,3)$$
$$H+O_2+M \rightarrow HO_2+M, \qquad (H.R\,10)$$
$$H+HO_2 \rightarrow OH+OH, \qquad (H.R\,12)$$
$$OH+H+M \rightarrow H_2O+M, \qquad (H.R\,9)$$

and

$$OH+OH \rightarrow O+H_2O. \qquad (H.R\,4)$$

In addition, the following two reactions have fairly large reaction rates under the stoichiometric or the rich conditions;

$$OH+OH+M \rightarrow H_2O_2+M, \qquad (H.R\,21)$$

and

$$H+H_2O_2 \rightarrow OH+H_2O. \qquad (H.R\,19)$$

The main combustion reactions, (H.R 5), (H.R 2), (H.R 3), (H.R 10) and (H.R 12), roughly keep a similar relation in their rates as that predicted in a stoichiometric hydrogen/air premixed flame[11], though their absolute rates are about 1/500 or less. All the reactions possess their maximum reaction rates in the vicinity of the surface with the stoichiometric composition. The main reaction zone is restricted to the region with the stoichiometric or the rich composition, that is, the region between 5 mm and 6 mm in radius. Reaction (H.R 5) is, however, exceptionally activated in a wide range of the equivalence ratio from 0.005 to 100000. This is caused by the wide presence of OH radicals even in the rich region as shown in Fig. 5. A large amount of the oxidizer and the high temperature activate the oxidation step of H_2 up to a large rate.

Hydroxyl radicals are supplied through the radial diffusion in the rich region. Reaction (H. R 4) proceeds to the reverse direction and produces OH radicals in the main reaction zone. This step is one of the predominant sources of OH radicals in the lean side.

Thermal energy is evolved, for the most part, in the rich side due to the activation of the reactions in this region, though the maximum heat release is attained at the surface of unity in the equivalence ratio. The region of heat release with a rate larger than 10 MJ/m³·s is spread out over a range from 4 mm to 6 mm in radius at this height. The heat release is ascribed predominantly to reaction (H. R 5), and also to reaction (H. R 10). The maximum heat-release rate at this height amounts to 50 MJ/m³·s at 6 mm in radius.

The distributions of the axial and the radial flow velocities at 10 mm in height are shown in Fig. 6. The axial velocity decreases gradually with an increasing radius in the central zone but steeply in the main reaction zone. The distrubution of the radial velocity indicates that the air is entrained at this height. The amount of oxygen supplied by the entrainment is approximately in the same order of magnitude as that of the axial diffusion, though it is about 1/10 to 1/100 of the radial diffusion.

The intersections of the flame with a height larger than 10 mm also have similar distributions of temperatures, flow velocities and concentrations except

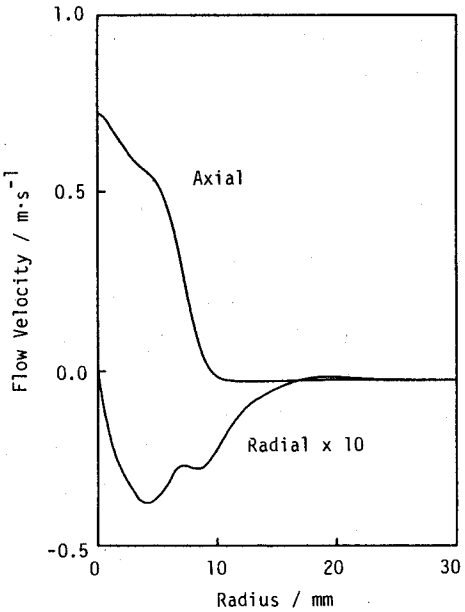

Figure 6. Distribution of radial and axial velocities at 10 mm in height.

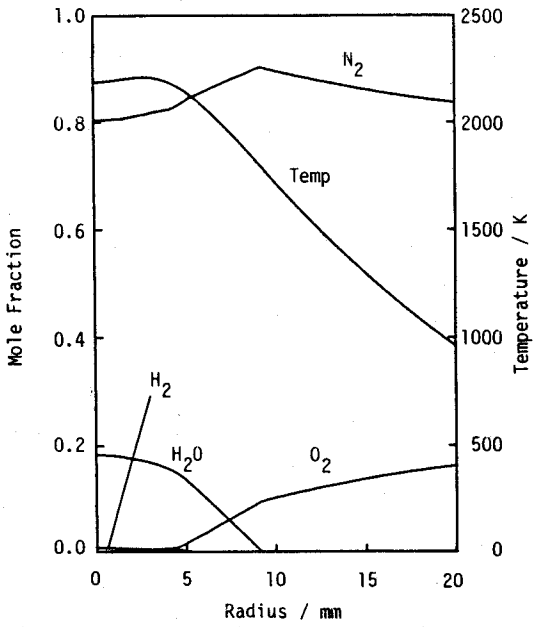

Figure 7. Radial profiles of temperature and concentrations of stable species at 40 mm in height.

those of fuel, the reaction products and nitrogen. At about 40 mm in height, the fuel has been consumed down to 0.01 in mole fraction even along the center line as shown in Fig. 7. Most of the chemical reactions have, therfore, been completed by the time the gas mixture flows to this height. The axial flow velocity is widespread in a range from 1.12 m/s to 0.05 m/s and follows approximately a Gaussian distribution. The radial flow of the gas is directed slightly outside with the radial velocity less than 0.01 m/s. The main oxidation step of H_2 by OH radicals has a fairly large reaction rate in the lean side. Its rate is about 1/10 of that at 10 mm in height.

The temperature must be raised up to a certain value within a fairly small time interval even in a low-temperature region to hold a flame at burner edges. This is the most severe condition for steady combustion of a diffusion flame of the type simulated in this investigation, because there is no recirculation zone in this flame as described above. One of the roles assigned to the analyses of the mechanism of stable combustion may be to elucidate how the temperature rises particularly at the base of a flame.

At 2 mm in height, the main combustion reactions are not activated yet. The amount of H_2O is negligibly small. However, the production of HO_2 radicals and their decomposition, that is, reactions (H. R 10) and (H. R 12), exceptionally

occur in a small range of radius around 4 mm. These reactions are accompanied with heat release. Hydrogen atoms consumed through these reactions are supplied with the axial diffusion from the downstream region. Thus, enthalpy is carried into the region in the form of chemical energy instead of thermal energy. This situation is observed also in the simulation of the low-temperature rigion in a one-dimensional hydrogen/air premixed flame[11]. The temperature reaches the maximum value, 1160 K, just outside the burner wall. This temperature rise is mostly ascribed to the axial thermal conduction. It should be noted that the axial diffusion of H atoms and the axial conduction of thermal energy also play an important role in this flame. The boundary-layer approximation is not always valid in predicting the structure at the base of the flame.

The combustion reactions are initiated within a few milliseconds, and then considerable changes take place on the radial profiles of the temperatures and the concentrations between 2 mm and 3 mm in height. Figures 8 and 9 depict the radial profiles of the temperatures and the concentrations of stable species and those of active species at 3 mm in height, respectively. The predominant reactions at this height are reactions (H.R 5), (H.R 2) and (H.R 3). As indicated by the concentration profiles, these reactions take place at the

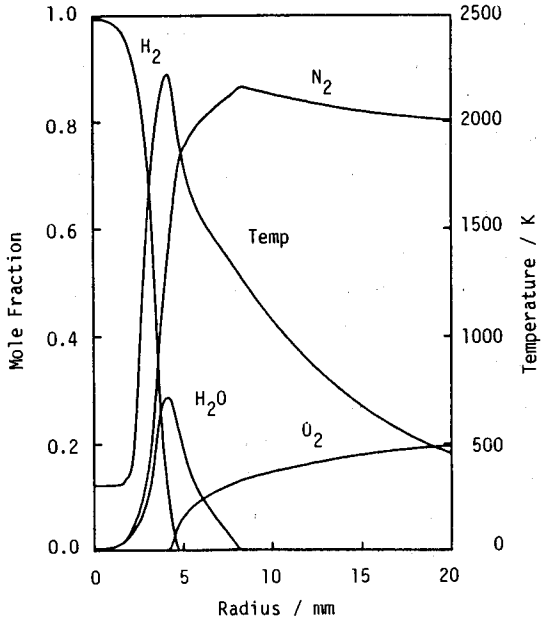

Figure 8. Radial profiles of temperature and concentrations of stable species at 3 mm in height.

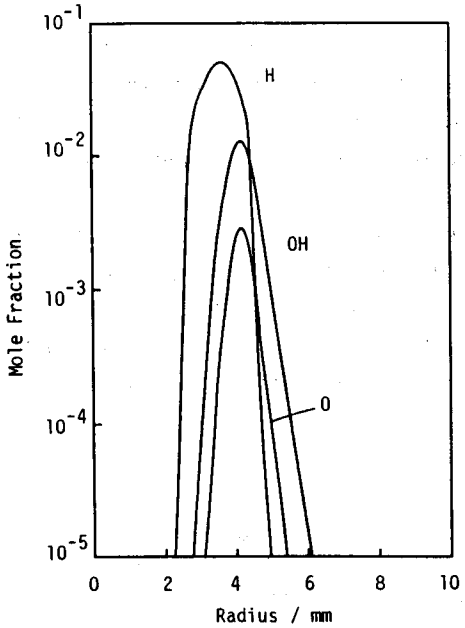

Figure 9. Radial profiles of concentrations of active species at 3 mm in height.

rich side with the equivalence ratio of around 0.1. A considerable amount of thermal energy is also released, and most of the heat release can be ascribed to reaction (H.R 5). The heat-release rate reaches more than 500 MJ/m³·s at about 4 mm in radius.

The flow toward the center line with the radial velocity of about 0.07 m/s is observed at the base of the flame. The environmental air is drawn inside due to this radial flow. At 3 mm in height, for instance, 10-50 % of oxygen is supplied with the radial convection, particularly in the region with a large heat release. Consequently, the radial flow contributes to the heat release through chemical reactions at the base of the flame, and the flame holding of this diffusion flame.

4. Concluding Remarks

A mathematical model, which was free from the boundary-layer approximation, and as precise as possible from the standpoint of chemical reactions, was established for hydrogen/air laminar diffusion flames. The simulation by means of this model gives the following conclusions on the flame structure and the

mechanism of flame holding:

1. The flame structure does not show large differences at positions higher than about 10 mm, though the reaction rate decreases with increasing height. The Burke–Schumann theory is proved to be valid. At 40 mm in height, most of the combustion reactions have been completed even in the vicinity of the center line.
2. At the base of the flame, some amount of oxygen is entrained into the main flow of the fuel due to the buoyancy of hydrogen, and mixes with the fuel in a short time. The fuel and the oxidizer behave as a premixed gas. The main combustion reactions of hydrogen, that is, reactions (H. R 5), (H. R 2) and (H. R 3) take place there. These chemical reactions hold the whole flame.

References

1) Miller, J. A. and Kee, R. J.: J. Phys. Chem. **81**, 2534 (1977)
2) Burke, S. P. and Schumann, T. E. W.: Ind. Eng. Chem. **20**, 998 (1928)
3) Gaydon, A. G. and Wolfhard, H. G.: Flames, 4th ed., Chapter 6, Chapman and Hall, 1979
4) Baulch, D. L., Drysdale, D. D., Horne, D. G. and Lloyd, A. C.: Evaluated Kinetic Data for High Temperature Reactions. Vol. 1, Butterworths, 1972
5) Jensen, D. E. and Jones, G. A.: Combust. Flame **32**, 1 (1978)
6) Heap, M. P., Tyson, T. J., Cichanowicz, J. E., Gershman, R. and Kau, C. J.: Sixteenth symposium (International) on Combustion, p. 535, The Combustion Institute, 1976
7) Baulch, D. L, Drysdale, D. D., Duxbury, J. and Grant, S.: Evaluated Kinetic Data for High Temperature Reactions, Vol. 3, Butterworths, 1976
8) Stull, D. R. and Prophet, H.: JANAF Thermochemical Tables, 2nd ed., U. S. Dept. of Commerce, 1971
9) Perry, R. H. and Chilton, C. H.: Chemical Engineer's Handbook, 5th ed., Section 3, McGraw-Hill, 1973
10) Patankar, S. V.: Numerical Heat Transfer and Fluid Flow, Chapter 3, Hemisphere Publishing Co., 1980
11) Fukutani, S. and Jinno, H.: Notes on Numerical Fluid Mechanics (N. Peters and J. Warnatz, Ed.), Vol. 6, P. 167, Vieweg, 1982